Available online at www.sciencedirect.com
SCIENCE DIRECT
Journal of Power Sources 154 (2006) 262–267
JOURNAL OF POWER SOURCES
www.elsevier.com/locate/jpowsour

Short communiction

Synthesis and electrochemical properties of $LiNi_{0.80}(Co_{0.20-x}Al_x)O_2$ ($x = 0.0$ and 0.05) cathodes for Li ion rechargeable batteries

S.B. Majumder, S. Nieto, R.S. Katiyar*

Department of Physics, University of Puerto Rico, San Juan, Apdo 23343, PR 00931-3343, USA

Received 16 February 2005; accepted 2 March 2005

Abstract

The effect of simultaneous cobalt as well as aluminum doping was studied to understand their effect on the phase formation behavior and electrochemical properties of solution derived lithium nickel oxide cathode materials for rechargeable batteries. The discharge capacities of $LiNi_{0.80}Co_{0.20}O_2$ and $LiNi_{0.80}Co_{0.15}Al_{0.05}O_2$ cathodes, measured at constant current densities of 0.45 mA cm^{-2} in the cut-off voltage range of 4.3–3.2 V, were 100 and 136 mAh g^{-1}, respectively. $LiNi_{0.80}Co_{0.15}Al_{0.05}O_2$ had better cycleability than the $LiNi_{0.80}Co_{0.20}O_2$ cathodes. The retention of undesirable Li_2CO_3 phase both in $LiNi_{0.80}Co_{0.20}O_2$ and $LiNi_{0.80}Co_{0.15}Al_{0.05}O_2$ cathodes was argued to be responsible for the relatively lower discharge capacity of these materials.

Keywords: Li ion batteries; Cathode materials; Electrochemical properties; Sol–gel synthesis

1. Introduction

Lithium nickel oxide has been considered as an alternative cathode material due to its higher discharge capacity (∼200 mAh g^{-1}) as compared to lithium cobalt oxides (140 mAh g^{-1}). However, before the commercial acceptance of lithium nickel oxide as cathode material, several material related shortcomings need to be solved. These problems and related research issues are summarized as follows [1–4]: (i) the cation disorder of Ni ions in the lithium site leads to a lithium deficient pristine material with the stoichiometry $(Li_{1-z}Ni_z^{2+})(Ni_z^{2+}Ni_{1-2z}^{3+})O_2$. During the electrochemical charging Ni^{2+} in the Li plane oxidized to Ni^{3+} state and the resulting structural distortion inhibits Li ion intercalation during first discharge resulting a huge polarization loss. Therefore, reduction of Ni^{3+} to Ni^{2+} during the cathode synthesis and the migration of Ni^{2+} ions in the Li^{1+} site need to be inhibited. (ii) Ni^{3+} (d^7) in its low spin $t_{2g}^6e_g^1$ configuration is prone to Jahn–Teller distortion and as a result the NiO_6 octahedra are locally distorted and the induced strain leads to the discontinuity to the particle–particle/particle–electrode contact, which eventually increases the electrode resistance and capacity fading. The capacity fading should be minimized by reducing the Jahn–Teller distortion. (iii) In its charged state, $Li_{1-x}NiO_2$ loses oxygen through an exothermic reaction. The rise in temperature is alarming especially when organic liquid electrolyte is used and its flash point is reached resulting a cell explosion. Additionally, with moderate rise in temperature the migration of divalent Ni ion is expedited from octahedral 3b site to 3a Li plane. Attempts should therefore be made to increase the thermal stability of lithium nickel oxide. (iv) Even when the pristine LNO is stoichiometric, during repeated cycling its layered rhombohedral structure is reported to be partially transformed into an electrochemically inactive spinel structure. It has been predicted by theoretical calculations [5] that in case of $LiMnO_2$, iso-structural to $LiNiO_2$, the layer to spinel transformation occurs in two steps, first the divalent Mn ion enters into an intermediate tetrahedral site before it enters the octahedral Li 3a site, followed by the migration of Li ion in another vacant tetrahedral sites.

* Corresponding author. Tel.: +1 787 751 4210; fax: +1 787 764 2571.
E-mail address: rkatiyar@rrpac.upr.clu.edu (R.S. Katiyar).

0378-7753/$ – see front matter © 2006 Published by Elsevier B.V.
doi:10.1016/j.jpowsour.2005.03.186

In the second step, the local arrangements of migrated Li and Mn ions leads to the formation of irreversible spinel structure through several other intermediate structures. The structural transformation with repeated cycling leads to capacity fading due to the loss of intercalating Li contents of the pristine material. In order to improve the capacity retention, therefore, the layered rhombohedral to spinel transformation should be inhibited.

It remains a major challenge to synthesize phase pure LNO without the Ni and Li cationic disorder. Although both LNO and LMO are iso-structural with $NaFeO_2$ type $LiCoO_2$, the problem of Ni and Mn ion migration is severe in LNO and LMO even at ∼50 °C and room temperature, respectively, while on the other hand the Co ion hardly migrates to Li plane even at higher temperature. A plausible explanation has been reported in literature by calculating the crystal field stabilization energies of Mn^{2+}, Ni^{2+} and Co^{2+} cations in octahedral and tetrahedral sites. For the low spin configurations of Ni^{3+} ($3d^7$), Co^{3+} ($3d^6$) and high spin configuration of Mn^{3+}($3d^4$) in octahedral configuration, the octahedral site stabilization energy (OSSE) (the difference between the crystal field stabilization energy (CFSE) between the CFSE values of octahedral and tetrahedral coordination) increases in the order of Mn^{3+} (−4.22 Dq) < Ni^{3+} (−12.67 Dq) < Co^{3+} (−21.33 Dq) [6]. A larger OSSE value for Co^{3+} ions makes the migration of Co ions via the tetrahedral site difficult, whereas a comparatively lower OSSE for Ni and Mn ions make such migration kinetically favorable at slightly elevated and room temperature, respectively. To stabilize the layered hexagonal structure of $LiNiO_2$, therefore we have substituted part of Ni^{3+} with Co^{3+} to synthesize $LiNi_{0.80}Co_{0.15}O_2$ by a cost effective solution based route. Several recent research reports have indicated that during charging, Ni^{3+} is oxidized to Ni^{4+} state (whereas the valence state of Co^{3+} remains invariant) and electrode material becomes unstable in the oxidized state [1,4,7]. To impart better stability of the deintercalation cathode we have also synthesized Co and Al co-doped $LiNi_{0.80}Co_{0.15}Al_{0.05}O_2$ cathodes by solution based route. The structural and electrochemical characteristics of these cathode materials have been compared to establish that the co-doped cathodes exhibit better electrochemical performance.

2. Experimental

$LiNi_{0.80}Co_{0.20}O_2$ (LNCO) and $LiNi_{0.80}Co_{0.15}Al_{0.05}O_2$ (LNCAlO) powders were synthesized by chemical solution route using lithium acetate, nickel acetate, cobalt acetate and aluminum nitrate as precursor materials. For this purpose, stoichiometric metallic salts were dissolved separately in 2-ethyl-hexanoic acids at 50 °C. Finally they were mixed together with continuous stirring at 50 °C for 1 h to make a homogeneous precursor solution. The solution was dried overnight at 110 °C to form precipitate. The dried precipitate was calcined at 450 °C for 2 h in air to oxidize the organic impurities. The resultant powders were calcined in the temperature range of 550–700 °C for 15 h for crystallization. The phase formation behavior of the calcined powder was characterized by XRD using Cu Kα radiation in the 2θ ranges of 15°–75°. The selected diffraction peaks were scanned at a slow scanning speed of 0.6° min^{-1}. From the recorded XRD pattern, the accurate peak position (2θ), integrated intensities, as well as the full-width at half maxima (FWHM) (β) of each slow scanned diffraction peaks were estimated by fitting them with Pearson VII amplitude function using a commercial peak fit software. These values were used to calculate the crystallite size and lattice strain of the synthesized powder using Williamson Hall equation [8]. From the fitted data, the lattice parameters of the synthesized powders were also calculated using a least square method.

The electrochemical characteristics of the synthesized cathode powders were carried out in a two-electrode test cell kept inside a glove box. A composite cathode was prepared as a mixture of the calcined oxide powder, carbon black and poly-vinylidene fluoride (in the weight ratio of 80:10:10), emulsion with *n*-methyl-2-pyrrolidone in a slurry, painted on aluminum foil and vacuum dried overnight at 100 °C. Lithium metal foils were used as counter and reference electrodes. The 1 M $LiPF_6$, in a 1:1 (w/w) mixture of ethylene carbonate and dimethyl carbonate (DMC) was used as electrolyte. The Celgard 2400 was used as separator between anode and cathode. A computer controlled potentiostat/galvanostat system [consisting a PC 750.4 controller and PHE 200 software (from Gamry Instruments)] was used for cyclic voltammetry and charge–discharge measurements. The CV plots were recorded at a scan speed of 0.2 mV s^{-1} in a voltage range of 4.2–3.2 V. Charge–discharge measurements at ambient temperature were performed in a voltage range of 4.2–3.2 V at a constant current density of 0.45 mA cm^{-2}.

3. Results and discussions

Fig. 1 shows the X-ray diffractograms of $LiNi_{0.80}Co_{0.20}O_2$ powders calcined at: (a) 550, (b) 650 and (c) 700 °C for 15 h. The X-ray diffractograms were indexed as α-$NaFeO_2$ type structure having a space group *R*-3*m*. As reported in the literature, higher intensity ratio of the (0 0 3) and (1 0 4) diffraction peaks as well as the clearer splitting of the (0 0 6)/(1 0 2) and (1 0 8)/(1 1 0) diffraction peaks indicate improved layered structure [9–11]. As shown in the fast scanned (3 min^{-1}) XRD patterns, LNCO powder, calcined at 700 °C for 15 h (Fig. 1a) exhibited better hexagonal layered structure as compared to the powders calcined at relatively lower temperatures (Fig. 1b and c). The splitting of the 1 0 1/0 0 6/1 0 2 as well as 1 0 8/1 1 0 diffraction peaks are better resolved in the slow scanned XRD patterns (Fig. 1d and e, respectively). These diffraction peaks were de-convoluted with Pearson VII amplitude function using commercial software and the resultant fit as well as the de-convoluted peaks is also shown in the figures. The other diffraction peaks, indexed in Fig. 1c, were also

Table 1
Structural parameters of lithium nickel cobalt oxide based cathode

Composition	a_H (Å)	c_H (Å)	c_H/a_H	$I_{int(300)}/I_{int(104)}$	R factor	Cell volume (Å^3)
$LiNi_{0.8}Co_{0.2}O_2$	2.86	14.16	4.95	1.22	0.07	100.50
$LiNi_{0.8}Co_{0.15}Al_{0.05}O_2$	2.86	14.17	4.95	1.12	0.08	100.63

slow scanned and fitted with Pearson VII amplitude function and the fitted 2θ positions were used to calculate the lattice parameter of the calcined powders. Fig. 2 shows the XRD patters of LNCAlO powders calcined at: (a) 650 and (b) 700 °C for 15 h. The de-convoluted slow scanned 1 0 1/0 0 6/1 0 2 as well as 1 0 8/1 1 0 diffraction peaks is shown in Fig. 2c and d, respectively. The other indexed peaks in Fig. 2b were also slow scanned and from the fitted peaks the accurate 2θ positions were obtained to calculate the lattice parameters of the LNCAlO powder. Table 1 summarizes the estimated structural parameters of LNCO as well as LNCAlO powders calcined at 700 °C for 15 h. As shown in Table 1 the integrated intensity ratio of I_{003}/I_{104} diffraction peaks are slightly higher in LNCO (∼1.22) as compared to LNCAlO (∼1.12) powders, which indicate better cation ordering in undoped powder. Additionally the calculated lower R factors (∼0.07) (defined by intensity ratio of $I_{006}/(I_{101}+I_{102})$) in both the powders also indicate excellent hexagonal ordering. The lower unit cell volume (∼100 Å^3) also indicates better cation ordering in the pristine powders. The calculated lattice parameters of the LNCO powders do not significantly altered due to Al doping and the calculated 'c', 'a' and c/a ratio matches well with the existing literature reports [11–12]. The crystallite size and the lattice strain calculated for $LiNi_{0.8}Co_{0.2}O_2$ and $LiNi_{0.8}Co_{0.15}Al_{0.05}O_2$ powders were 156, 0.0017 and 145, 0.0018 nm, respectively. Close inspection of the Fig. 1a–c and Fig. 2a and b reveals the presence of impurity phases (marked as '*') in both the powders. The contents of the impurity phases are prominent in powders calcined at lower temperatures (Fig. 1a) and these reduce with the increase in calcinations temperature (Fig. 1b and c). The inset in Fig. 1 shows the slow scanned XRD of this impurity phase in the LNCO powder calcined at 550 °C for 15 h. The impurity phase was indexed as Li_2CO_3. Many other researchers have also detected the presence of $LiCO_3$ in undoped $LiNiO_3$ and Co and Al co-doped $LiNiO_3$ cathode materials [13–16]. The solution prepared powders are very reactive presumably due to their finer particle size (<100 nm) and therefore they can react with atmospheric CO_2 and O_2 to form Li_2CO_3 layer at the surface of the particles.

Cyclic voltammetry (CV) experiments of LNCO as well as LNCAlO composite cathodes were performed to detect the electrochemical reaction(s) during charge–discharge cycling. Pure $LiNiO_2$ was reported to exhibit three phase transitions (hexagonal to monoclinic, monoclinic to hexagonal and hexagonal to hexagonal phases) during the Li extraction and insertion, which can be detected by corresponding anodic

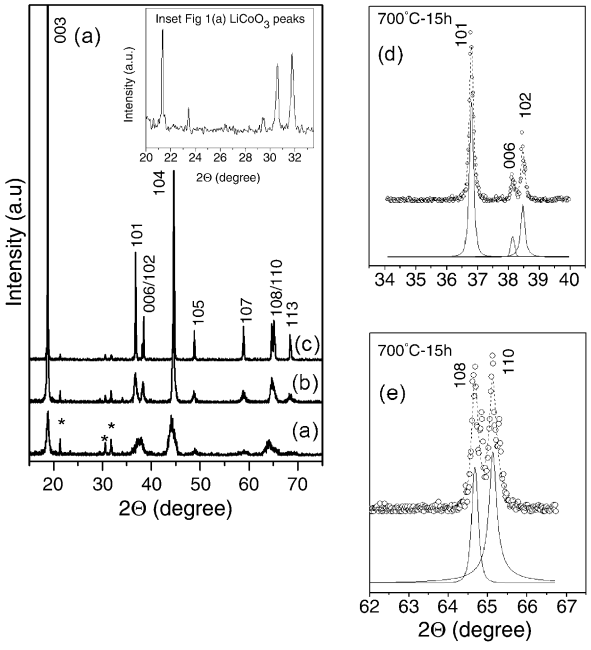

Fig. 1. X-ray diffractograms of $LiNi_{0.80}Co_{0.20}O_2$ powders calcined at: (a) 550 °C, (b) 650 °C and (c) 700 °C for 15 h in air. The slow scanned XRD pattern (circle), fitted curve (dashed line) and the resolved peaks (solid line) for (1 0 1)/(0 0 6)/(1 0 2) and (1 0 8)/(1 1 0) peaks are shown in (d and e), respectively.

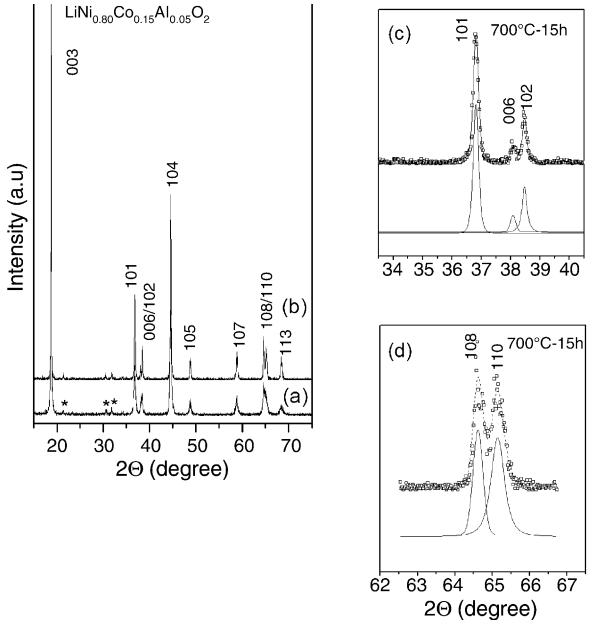

Fig. 2. X-ray diffractograms of $LiNi_{0.80}Co_{0.15}Al_{0.05}O_2$ powders calcined at: (a) 650 °C and (b) 700 °C for 15 h in air. The slow scanned XRD pattern (circle), fitted curve (dashed line) and the resolved peaks (solid line) for (1 0 1)/(0 0 6)/(1 0 2) and (1 0 8)/(1 1 0) peaks are shown in (c) and (d), respectively.

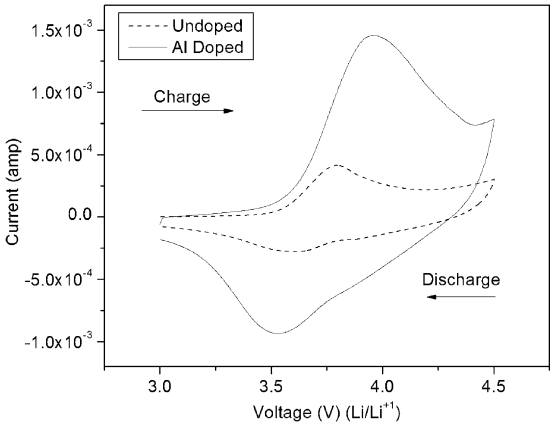

Fig. 3. Cyclic voltammograms of $LiNi_{0.80}Co_{0.20}O_2$ and $LiNi_{0.80}Co_{0.15}Al_{0.05}O_2$ composite cathodes.

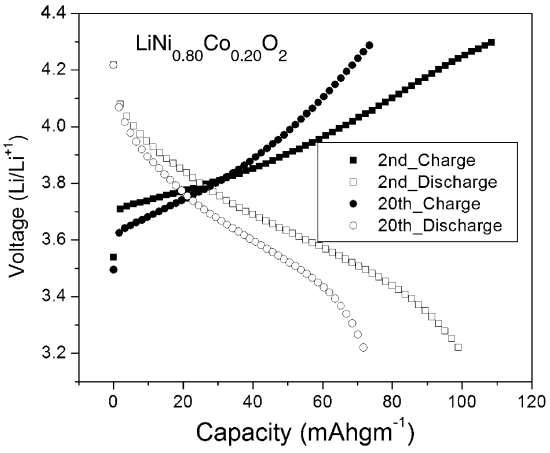

Fig. 4. Charge discharge profiles of $LiNi_{0.80}Co_{0.20}O_2$ composite cathode after 2nd and 20th cycles in the cut-off voltage range of 4.2–3.2 V.

and cathodic peaks during CV measurements [17]. Fig. 3 compares the cyclic voltammograms of LNCO and LNCAlO cathodes. As shown in the figure, for both the samples, the occurrence of only one broad peak in oxidation region and a broad minimum in the reduction region indicates a single-phase reaction takes place during the charge–discharge cycling. In contrast, Han et al. [18] observed the presence of three peaks in the CV of $LiNi_{0.8}Co_{0.20}O_2$ cathode, which arises from multiple phase transitions during charge–discharge cycle. Increased Al doping content (up to 5 at% replacing Co) were reported to merge these multiple peaks into a single one which indicates that the multiple phase transitions are inhibited due to Al doping. Thus, in case of our solution prepared LNCO powder, we have observed that Co doping alone could suppress the multiple phase transition observed during the charge–discharge of $LiNiO_2$ cathode materials. The anodic peak of the LNCO cathode shifts from 3.79 to 3.95 V in LNCAlO cathode, whereas the corresponding cathodic peak shifts to lower voltage, i.e, from 3.6 to 3.5 V. The observed peak shift in the Al doped sample indicates structural modification of the hexagonal ordering of LNCO cathode induced by Al doping.

Figs. 4 and 5 show the charge and discharge profiles of LNCO and LNCAlO cathodes after 2nd and 20th cycles, respectively, in the cut-off voltage 4.2–3.2 V. The discharge capacity of LNCO and LNCAlO cathodes after 2nd cycles are 100.05 and 135.91 mAh g^{-1}, respectively. Thus, better discharge capacity is obtained in Al doped LNCO cathodes. After 20th charge–discharge cycles the discharge capacities for the LNCO and LNCAlO cathodes were 72.47 and 110.51 mAh g^{-1}, respectively. Hence, the capacity retention of Al doped cathode (~82%) was also better as compared to LNCO cathodes (~63%). Table 2 compares the electrochemical characteristics of $LiNi_{1-x}Co_xO_2$ based cathodes prepared by different processing routes. As shown in the table, since different load currents are used in the capacity measurements, it is difficult to make any effective comparison between the discharges capacities of LNCO based cathodes prepared in different laboratories. The discharge capacity of the solution derived LNCO based cathodes of the present work is lower as compared to recent literature reports. However, as compared to LNCO cathode, 5% Al doped LNCAlO cathodes exhibit better discharge capacity and capacity retention after charge–discharge cycling. We feel that the observed lower discharge capacity is due to the coexistence of Li_2CoO_3 with the desired hexagonal layered phase of these cathode materials. As mentioned earlier, the presence of lithium carbonate on the surface of active cathode materials (such as $LiNiO_2$) has been reported in many literature reports.

Recently, Zhuang et al. [16] reported a detailed study on the effect of Li_2CO_3 on the discharge capacity, rate capability and capacity retention of $LiNi_{0.80}Co_{0.15}Al_{0.05}O_2$ cathodes. The formation of a continuous film of about 10 nm thick Li_2CO_3 was detected by high-resolution TEM measurements on $LiNi_{0.8}Co_{0.15}Al_{0.05}O_2$ particles exposed in air. The formation of Li_2CO_3 was explained due to reaction of atmospheric carbon di-oxide with lithium oxide residue/or with Li from the active cathode material. The presence of Li_2CO_3 layer would increase the impedance of the cathode since it has inferior electronic as well as ionic conductivities

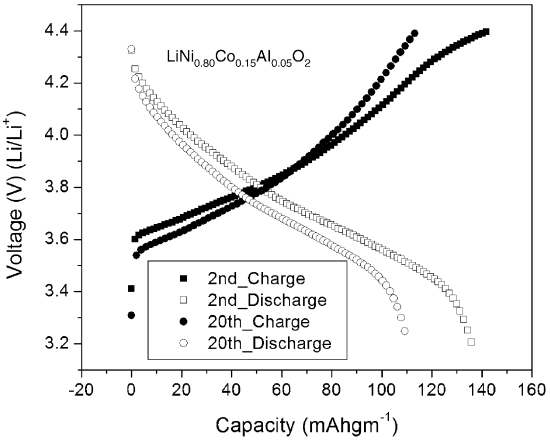

Fig. 5. Charge discharge profiles of $LiNi_{0.80}Co_{0.15}Al_{0.05}O_2$ composite cathode after 2nd and 20th cycles in the cut-off voltage range of 4.2–3.2 V.

Table 2
Comparison of the electrochemical characteristics of $LiNi_{1-x}Co_xO_2$ based cathodes prepared by different processing techniques

Composition	Synthesis route	Discharge capacity ($mAh\,g^{-1}$) (voltage range, V)	Rate	% Capacity retention (no. of cycles)	Reference
$LiNi_{0.8}Co_{0.2}O_2$, $LiNi_{0.8}Co_{0.15}Al_{0.5}O_2$	Sol–gel	182 (4.3–3), 161 (4.3–3)	C/5	51 (50)	[18]
$LiNi_{0.8}Co_{0.2}O_2$	Powder obtained from Merck	193 (4.3–3.3)	C/16	67 (20)	[3]
$LiNi_{0.8}Co_{0.2}O_2$	Solution combustion	154 (4.2–3)	C/10	94 (20)	[11]
$LiNi_{0.85}Co_{0.15}O_2$, $LiNi_{0.85}Co_{0.12}Al_{0.3}O_2$	Solution based technique	180 (4.2–3.2), 170 (4.2–3.2)	C/5	90 (20) 98 (20)	[4]
$LiNi_{0.8}Co_{0.15}Al_{0.05}O_2$	Obtained from Fuji	65(4–3)	C/6	–	[16]
$LiNi_{0.8}Co_{0.2}O_2$, $LiNi_{0.8}Co_{0.15}Al_{0.5}O_2$		100 (4.2–3.2), 136 (4.2–3.2)	$0.45\,mA\,cm^{-2}$	63 (20) 82 (20)	This work

and therefore it affects adversely the discharge capacity, rate capability and the capacity retention characteristics. Thus, a discharge capacity as low as $25\,mAh\,g^{-1}$ has been reported (discharged at C/6 rate) in the case of air exposed $LiNi_{0.8}Co_{0.15}Al_{0.05}O_2$ cathode as compared to the capacity $\sim 65\,mAh\,g^{-1}$ in case of freshly prepared cathodes discharged at the same rate. As mentioned earlier, in the present work we have also detected the existence of Li_2CO_3 phase both in LNCO as well as LNCAlO calcined powders by slow scanned XRD analyses. Although at this stage it is not clear how this secondary phase is distributed in the active matrix, certainly it affects the discharge capacity of these cathode materials. Irrespective of the presence of this secondary phase, Al doping shows the signature of the betterment of the capacity retention in LNCAlO cathode materials. Probably during the charge–discharge cycling Al^{3+} ions migrate in between the NiO_6 layer forming the sol called pillar structure to impart the structural stability of the hexagonal structure and thereby improve the cycleability of the cathode materials [19]. Studies are in progress to understand these issues better.

4. Conclusions

In the present work we have compared the phase formation behavior and electrochemical properties of solution derived $LiNi_{0.80}Co_{0.20}O_2$ and $LiNi_{0.85}Co_{0.15}Al_{0.05}O_2$ cathode materials for Li ion rechargeable batteries. From the occurrence of a single broad oxidation/reduction peak in cyclic voltammograms we inferred that the cobalt doping contents (20 at%) were sufficient to suppress the multiple structural phase transitions observed in $LiNiO_2$ cathode materials. The discharge capacity of $LiNi_{0.80}Co_{0.20}O_2$ and $LiNi_{0.85}Co_{0.15}Al_{0.05}O_2$ cathodes was measured to be 100 and $136\,mAh\,g^{-1}$ measured at a constant current densities of $0.63\,mA\,cm^{-1}$ in the cut-off voltage range of 4.3–3.2 V. Five atomic percent of Al doping were found to improve the capacity retention from 63% in $LiNi_{0.80}Co_{0.20}O_2$ cathode to 82% in case of $LiNi_{0.85}Co_{0.15}Al_{0.05}O_2$ cathode materials. Relatively lower discharge capacity was achieved in the cathodes synthesized in the present work as compared to those reported in open literatures. It has been argued that the coexistence of secondary Li_2CO_3 with the desired hexagonal layered phase of these materials are responsible for poor discharge capacity of these materials. Studies are in progress to eliminate the occurrence of this secondary phase to further improve the electrochemical characteristics of these synthesized cathodes.

Acknowledgments

The above research work was partially supported by the research grants from DiE (# DE-FG02-01ER45868) and NASA (#NAG3-2676) Glenn Research Center. XRD measurements were carried out utilizing the facilities at the Materials Characterization Center (MCC) of UPR.

References

[1] C. Delmas, L. Croguennec, Mater. Res. Soc. Bull. (2002) 608.
[2] I. Nakai, T. Nakagome, Electrochem. Solid-State Lett. 1 (1998) 259.
[3] H. Omanda, T. Brousse, C. Marhic, D.M. Schleich, J. Electrochem. Soc. 151 (2004) A922.
[4] A.M. Kannan, A. Manthiram, J. Electrochem. Soc. 150 (2003) A349.
[5] J. Reed, G. Ceder, A.V.D. Ven, Electrochem. Solid-State Lett. 4 (2001) A78.
[6] S. Choi, A. Manthiram, J. Electrochem. Soc. 149 (2002) A1157.
[7] T. Ohzuku, T. Yanagawa, M. Kouguchi, A. Ueda, J. Power Sources 68 (1997) 131.
[8] G.K. Williamson, W.H. Hall, Acta Metall. 1 (1953) 222.
[9] T. Ohzuku, A. Ueda, M. Nagayama, Y. Iwakoshi, H. Komori, Electrochim. Acta 38 (1993) 1159.
[10] B.J. Hwang, R. Santhanam, C.H. Chen, J. Power Sources 114 (2003) 244.
[11] P. Periasamy, H.S. Kim, S.H. Na, S.I. Moon, J.C. Lee, J. Power Sources 132 (2004) 213.
[12] R. Moshtev, P. Zlatilova, I. Bakalova, S. Vassilev, J. Power Sources 4840 (2002) 1.
[13] D. Aurbach, K. Gamolsky, B. Markovsky, G. Salitra, Y. Gofer, U. Heider, R. Oesten, M. Schmidt, J. Electrochem. Soc. 147 (2000) 1322.
[14] A.M. Andersson, D.P. Abraham, R. Haasch, S. MacLaren, J. Liu, K. amine, J. Electrochem. Soc. 149 (2002) 6917.

[15] H.K. Kim, T.Y. Seong, W. Cho, Y.S. Yoon, J. Power Sources 109 (2002) 178.
[16] G.V. Zhuang, G. chen, J. Shim, X. Song, P.N. Ross, T.J. Richardson, J. Power Sources 134 (2004) 293.
[17] K. Lee, K. Kim, in: R.A. Marsh, Z. Ogumi, J. Prakash, S. Surampudi (Eds.), Lithium Batteries, Proceeding, The Electrochemical Society Proceeding Series, vol. 99-25, Honolulu, Hawaii, Fall, 1999, p. 257.
[18] C.J. Han, J.H. Yoon, W.I. Cho, H. Jang, J. Power Sources 136 (2004) 132.
[19] H.S. Kim, T.K. Ko, B.K. Na, W.I. Cho, B.W. Chao, J. Power Sources 138 (2004) 232.